preferential occupation of d_{xz}- and d_{yz}-type orbitals. This corresponds to the presence, on the difference maps, of a deformation density between directions joining a pair of neighbouring ions, V^{2+} and F^-.

The main source of error in these parameters is likely to be the assumption that the asphericity of the 3d electrons is the only contribution to the observed difference density.

In the case of crystal II, the values of α_2 and α_3 yielding a minimum of χ^2 are negative. This can be attributed to the constraint imposed on the sum of the α_i ($i=1$ to 5): the best fit tends to occur at the highest possible values of α_4 and α_5, and this apparently forces α_2 and α_3 to be negative. Since the definition of the parameters α_i shows that negative values are meaningless, α_2 and α_3 were taken to be zero.

The results obtained from the multipole analysis show that only two multipole amplitudes, C_0 and C_{20}, are significant. C_0 is a measure of the spherical contribution of the 3d electrons to the scattering factor. The aspherical electron density associated with the multipole P_2^0, whose amplitude is C_{20}, shows positive lobes directed along the Z axis (Stewart, 1976). Hence, the negative value obtained for C_{20} evidences a deficiency of charge density along the directions $V^{2+}-F^-$. This is in agreement with the conclusion derived from the analysis based on 3d wave functions: the 3d electrons tend to avoid directions joining a pair of ions, V^{2+} and F^-.

It may be inferred from the above considerations that no significant degree of covalency could be detected in vanadium difluoride.

We thank Dr P. J. Brown at the Institute Laüe-Langevin, Grenoble, for stimulating discussions and for allowing us to use some of her programs. We also thank Mrs L. C. R. Andrade for critical comments on this work.

We are indebted to the Cultural Service of the German Federal Republic Embassy, the Deutsche Akademischer Austauschdienst (DAAD) and the German Agency for Technical Cooperation (GTZ) for the offer of a CAD-4 automatic diffractometer which enabled the experimental work to be carried out.

References

Abragham, A. & Bleaney, B. (1970). *Electron Paramagnetic Resonance of Transition Ions.* Oxford: Clarendon Press.

Almeida, M. J. M. de & Costa, M. M. R. (1985). *Port. Phys.* **16**, 181-190.

Andrade, L. C. R., Costa, M. M. R. & de Almeida, M. J. M. (1983). Proc. I Simpósio Ibérico de Física da Matéria Condensada, Lisboa, 1983.

Clementi, E. & Roetti, C. (1974). *At. Data Nucl. Data Tables,* **14**(3), 4.

Condon, E. U. & Shortley, G. H. (1963). *The Theory of Atomic Spectra.* Cambridge Univ. Press.

Frenz, B. A. (1983). *Enraf-Nonius Structure Determination Package; SDP Users Guide,* version 1.0. Enraf-Nonius, Delft, The Netherlands.

International Tables for X-ray Crystallography (1974). Vol. III. Birmingham: Kynoch Press. (Present distributor D. Reidel, Dordrecht.)

North, A. C. T., Phillips, D. C. & Mathews, F. S. (1968). *Acta Cryst.* **A24**, 351-359.

Schweitzer, J. (1980). *Electron and Magnetization Densities in Molecules and Crystals. NATO Advanced Study Institute Series,* edited by P. Becker. London and New York: Plenum Press.

Stevens, E. D. & Coppens, P. (1975). *Acta Cryst.* **A31**, 612-619.

Stewart, R. F. (1973). *J. Chem. Phys.* **58**, 1668-1676.

Stewart, R. F. (1976). *Acta Cryst.* **A32**, 565-574.

Wanklyn, B. M., Garrard, B. J. & Wondre, F. (1976). *J. Cryst. Growth,* **33**, 165-168.

Acta Cryst. (1987). **B43**, 352-356

Electron Density in Non-Ideal Metal Complexes. III.* Bis(hydrazine)bis(hydrazinecarboxylato)cobalt(II)

By E. N. Maslen and S. C. Ridout

Department of Physics, University of Western Australia, Nedlands, Western Australia 6009

(*Received* 11 *September* 1984; *accepted* 19 *January* 1987)

Abstract

The difference density near the Co atom in the title compound $[Co(CH_3N_2O_2)_2(N_2H_4)_2]$ is broadly similar to that in other transition-metal complexes. The d-electron maxima are farther from the nucleus than the corresponding peaks for low-spin cobalt(III) complexes. The plane containing four ligand N atoms has approximate fourfold symmetry. Other sections, with ligand atoms of different types, are less symmetrical. Differences in the heights of the d-electron maxima are consistent with a modulating effect of interactions with second-nearest-neighbour atoms in the hydrazinecarboxylato moiety. Near the two ligand

---

[*] Part II: Maslen, Spadaccini, Watson & White (1986).

0108-7681/87/040352-05$01.50

O atoms the lone-pair density is rather diffuse. Closer to the Co atom, the features attributable to residual $3d$ density have satellite maxima, which appear to be related to the departure from the ideal octahedral symmetry, providing evidence for hybridization of the one-electron states in this structure. Crystal data have been given by Maslen, Raston, Skelton & White [*Aust. J. Chem.* (1975), **28**, 739-744].

Introduction

The electron density near the octahedrally coordinated Co atoms in hexamminecobalt(III) hexacyanocobaltate(III) was studied experimentally by Iwata & Saito (1973). The difference density $\Delta\rho$ shows a transfer of $3d$ electrons from the e_g states, directed towards the ligating atoms, to the t_{2g} states, which maximize along the body diagonals. Similar results have been reported for complexes of other members of the first transition series such as KMF_3, with M = Mn, Co, Fe and Ni (Kijima, Tanaka & Marumo, 1981, 1983; Miyata, Tanaka & Marumo, 1983). $\Delta\rho$ maps for complexes of metals from the third transition series have similar characteristics, shown by the analyses of K_2PtCl_4 by Ohba, Sato, Saito, Ohshima & Harada (1983) and K_2PtCl_6 by Ohba & Saito (1984).

The packing for octahedral metal complexes resembles that in the corresponding ionic solids in having electropositive atoms in second-nearest-neighbour positions along the body diagonals, except where this is precluded by the shapes of the ligands. Typically, the lengths of the vectors to these second-nearest neighbours are within 0·3 Å of the sum of the metallic radii. This raises the question of whether this packing is due to nearest-neighbour forces only, or whether second-nearest-neighbour terms have a significant role.

Spackman & Maslen (1986) have shown that the classical electrostatic energies of overlapping but undeformed atoms give a good first-order estimate of interaction energy. For solids it is the first term in a perturbation expansion of the cohesive energy (Trefry, Maslen & Spackman, 1987). Typically the contribution of second-nearest-neighbour cation–cation terms, being more than one quarter of that from nearest-neighbour cation–anion interactions, is too large to be neglected.

A further indication of the significance of the second-nearest-neighbour interactions is the orientation of the t_{2g} maxima, which lie along the interatom vectors. It is well known that in solid transition metals there is a transfer of electrons from the $4s$ to the $3d$ subshell, first noted by Sternheimer (1950). For metal complexes the $\Delta\rho$ maps are consistent with the hypothesis that there is similar transfer of density into the $3d$ subshell along the lines of interaction between the transition metal and electropositive neighbours. Thus, while a ligating atom 'sees' a positively charged metal due to the depletion of density in the e_g state, a second-nearest-neighbour cation 'sees' a density distribution closer to that in metallic bonds.

To confirm this hypothesis involved differentiating between the effects of first- and second-nearest neighbours on the electron density. This is fundamentally difficult for high-symmetry structures with ideal geometry, for which the first- and second-nearest neighbours have closely related symmetries. In principle, the problem is more tractable in lower-symmetry structures, for which the degree of ideality for the first- and second-nearest-neighbour geometries differ. Given sufficient accuracy, the degree of ideality of the deformation density indicates the relative importance of the two types of interaction. If a large number of second-nearest-neighbour interactions contribute equally to the cohesive energy, however, it may be difficult to identify the features in the deformation density resulting from particular interactions. To reduce this problem, we focus on structures with a limited number of relatively strong second-nearest-neighbour terms.

Maslen, Spadaccini, Watson & White (1986) applied this technique to $Na_2Cu(CO_3)_2$. The ligand geometry in that complex is regular, but there are also a limited number of short asymmetrically disposed Cu–Na vectors in the crystal structure. The topography of the $\Delta\rho$ map, being irregular, cannot be explained in terms of square-planar geometry, but is compatible with a model in which Cu–Na interactions are significant. The results are supported by an earlier investigation of copper potassium carbonate by Maslen, Spadaccini & Watson (1983).

Interactions beyond the first coordination sphere contribute terms of modest size to the bonding Hamiltonian. There is also considerable variety among these second-nearest-neighbour interactions in different structures. Before conclusions derived from one or two analyses can be regarded as general, their validity for other structures must be demonstrated. We therefore seek cases in which the significance of second-nearest-neighbour interactions can be tested.

A transition-metal complex with a bidentate ligand of small bite provides a suitable test. The ligand atoms at intermediate sites in the ligand chain are constrained to be close to the metal atom. The bidentate ligand inhibits the approach of other groups, so close second-nearest-neighbour atoms occur only within the ligand. A suitable structure is that of bis(hydrazine)bis(hydrazinecarboxylato)cobalt(II) determined by Maslen, Raston, Skelton & White (1975) (Fig. 1). The Co atom, which is in the high-spin state, occupies a centre of symmetry in the structure. Four of its nearest neighbours are N atoms, and the other two are O atoms. The intensity measurements, for which details are given in Table 1, were originally for the purposes of structure determination only. However the reflection profiles were uniform, and the

Table 1. *Crystal data and details of refinement*

$[Co(N_2H_4)_2(NH_2NHCO_2)_2]$, $M_r = 237{\cdot}12$, monoclinic, $P2_1/a$, $a = 9{\cdot}551\,(2)$, $b = 7{\cdot}352\,(2)$, $c = 8{\cdot}110\,(1)$ Å, $\beta = 122{\cdot}38\,(1)°$, $V = 480{\cdot}9\,(2)$ Å^3, $Z = 2$, $D_x = 1{\cdot}886$ g cm^{-3}, $\lambda(\text{Mo } K\alpha) = 0{\cdot}71069$ Å, $\mu = 18{\cdot}7$ cm^{-1}, $F(000) = 258$, $T = 295$ K
Cell from 15 reflections with $40 < 2\theta < 51°$
Prism-shaped crystal, dimensions $0{\cdot}20 \times 0{\cdot}18 \times 0{\cdot}14$ mm
Syntex $P\bar{1}$ diffractometer, ω–2θ scan
7304 measured intensities reduced to 4985 unique reflections by statistical averaging
$R_{\text{int}} = 0{\cdot}015$
$0 \leq h \leq 20, 0 \leq k \leq 15, -17 \leq l \leq 14, 0 \leq 2\theta \leq 100°$
Standard reflection $60\bar{1}$ measured every 50 reflections
Absorption correction range 1·25 to 1·41
Atomic scattering factors and dispersion corrections from *International Tables for X-ray Crystallography* (1974)
Refinement based on $|F|$
Weights $1/\sigma^2(|F|)$
Variance from counting statistics but modified for primary beam fluctuation by calibration from the standard reflection
$R(F) = 0{\cdot}057$
$wR(F) = 0{\cdot}031$
$S = 1{\cdot}573(16)$

intensities of repeat measurements for an inner set of reflections agreed within limits predicted from the counting statistics. The F_o *vs* F_c agreement indicated that the data were unaffected by extinction. Accordingly the data processing and structure refinement were repeated with the expectation that useful information on the charge density might be obtained.

Structure refinement

Table 2. *Cobalt environment – interatomic distances and interatom energies calculated as in Spackman & Maslen* (1986)

Vector	Distance (Å)	Energy (eV)
Co–O(1)	2·062(1)	−1·83
Co–N(3)	2·174(1)	−1·59
Co–N(2)	2·193(1)	−1·52
Co C	2·866(1)	−0·40
Co N(1)	2·904(1)	−0·28
Co N(4)	3·140(1)	−0·16

Table 3. *Atomic charges, as defined by Hirshfeld* (1977)

Atom	Charge	Atom	Charge
Co	0·05(2)	H(1)	0·07(2)
O(1)	−0·29(2)	H(2)	0·05(2)
O(2)	−0·35(2)	H(21)	0·08(2)
C	0·24(2)	H(3)	−0·03(2)
N(1)	0·06(2)	H(31)	0·04(2)
N(2)	0·08(2)	H(4)	0·06(2)
N(3)	0·02(2)	H(41)	−0·02(2)
N(4)	−0·03(2)		

Least-squares refinement of the structure was continued until $\Delta/\sigma < 0{\cdot}01$. Details are included in Table 1.* Distances from Co to atoms in the ligating groups are listed, along with the corresponding free-atom electrostatic interaction energies, in Table 2. The atom–atom energies were evaluated as described by Spackman & Maslen (1986). The distance from Co to C is about 0·5 Å longer than the 2·3 Å expected for a bonded high-spin Co–C bond length, but the electrostatic energy of −0·4 eV is appreciable when compared with the −1·3 eV expected for a bonded contact.

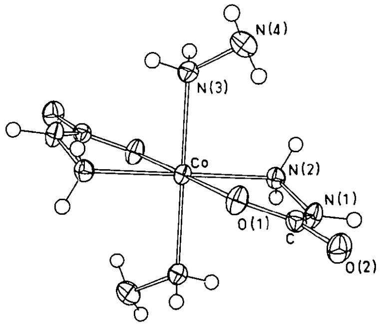

Fig. 1. The molecular geometry of bis(hydrazine)bis(hydrazinecarboxylato)cobalt(II).

Electron density

A residual electron-density map was evaluated. $\sigma(\Delta\rho)$, included for the benefit of those who believe it to be a useful indication of accuracy, was calculated by the method of Rees (1977) to be 0·11 e Å^{-3}. Atomic charges for the structure were determined by the stockholder method of Hirshfeld (1977) using a computer program *PARTN* (Chantler, 1985) compatible with the *XTAL* system (Stewart & Hall, 1985). The atomic charges, given in Table 3, are consistent for each atomic type and within the range expected from charge-density studies on related materials. Since the integrated densities are reliable, the stronger features in the map should be significant.

The deformation density near the ligands has the characteristics expected of bonds involving first-row atoms. This is shown in Fig. 2, which contains the usual trigonal arrangement of peaks and hollows about the sp^2 C atom. There is other internal evidence for the reliability of the deformation density. The plane containing the Co and its four neighbouring N atoms is shown in Fig. 3(*a*). The N-atom lone pairs are associated with maxima, approximately 0·5 e Å^{-3} in height, and roughly 0·7 Å along the N–Co vector. The density near Co, which contains the largest features in the map, has approximate 4*mm* symmetry. The angle dependence of the features is as expected for residual 3*d* electron density. Along the Co–N vectors there are hollows associated with reduced

---

* Lists of structure factors, anisotropic thermal parameters and refined atomic parameters have been deposited with the British Library Document Supply Centre as Supplementary Publication No. SUP 43653 (22 pp.). Copies may be obtained through The Executive Secretary, International Union of Crystallography, 5 Abbey Square, Chester CH1 2HU, England.

occupancy, compared with the free atom, of the e_g states. On the bisectors of the angles between adjacent Co–N vectors there are maxima associated with increased occupancy for the t_{2g} states.

Whereas the angle dependence of these features is similar to that observed for low-spin cobalt(III) complexes, the radial dependence is quite different. In hexaamminecobalt hexacyanocobaltate (Iwata & Saito, 1973), the t_{2g} maxima are close to ($0{\cdot}4_5$ Å) and the e_g minima farther (0·6 Å) from the nucleus. In this structure the minima are closer ($0{\cdot}3_5$ Å) and the maxima farther removed (0·6 Å) from the Co nucleus. This is as predicted for the high-spin state of the Co atom. The exchange repulsions associated with the parallel spins enhance the density farther from the nucleus, contributing to the well known increase in bond length associated with the high-spin state.

The difference density in a section containing the Co, two N and two O atoms is shown in Fig. 3(*b*). One aspect of Fig. 3(*b*) at first appears anomalous. If the angles subtended by the ligand atoms at the central metal deviate from the ideal value of 90°, the *d*-electron peak is usually higher in the larger angle. [See, for example, Fig. 1 in Stevens & Coppens (1979).] The larger peak in Fig. 3(*b*) is in the smaller angle. However, the stronger t_{2g} peak lies on the vector between the Co atom and the C atom which is electropositive, having the highest positive charge of any atom in the structure as indicated by Table 3. This increased height and size of the t_{2g} peak directed towards the C atom is consistent with enhancement of 3*d* electron density along vectors joining pairs of electropositive atoms. It thus resembles that of the peaks along the Cu–Na vectors in $Na_2Cu(CO_3)_2$ described by Maslen *et al.* (1986). Further, the magnitude of the Co to C energy (Table 2) is commensurate with the difference in size of the t_{2g} peaks. It is relatively smaller than that in copper sodium carbonate, for which the asymmetry of the map is much greater. Thus the results of the analyses are consistent.

The electron density associated with the O atoms is less well defined than that near the N atoms. This is also characteristic of metal-oxygen bonds. For example, in copper sulfate pentahydrate (Varghese & Maslen, 1985) the density near the O atoms is smeared out in directions roughly normal to the metal-oxygen bonds.

The electron density between the Co atom and the oxygen lone pair is of particular interest. Peaks along the directions bisecting the Co–N and Co–O vectors, at approximately 0·6 Å from Co, are characteristic of *d* electrons. There is, however, a pair of weaker maxima lying between these and the oxygen lone-pair density. This is also consistent with results for other analyses with more redundancy in the data (Maslen, Ridout & Watson, 1987).

Satellite maxima have been observed for other transition-metal complexes with non-ideal geometry. Structures with special relevance are the set of nearly isomorphous spinels M_2SiO_4 (M a transition metal)

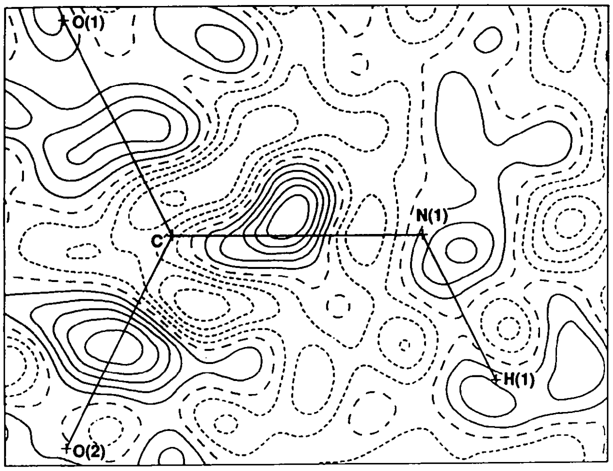

Fig. 2. Difference electron density in the plane of the carboxylate group in the hydrazinecarboxylato moiety. Contour interval 0·1 e Å^{-3}. Negative contours broken.

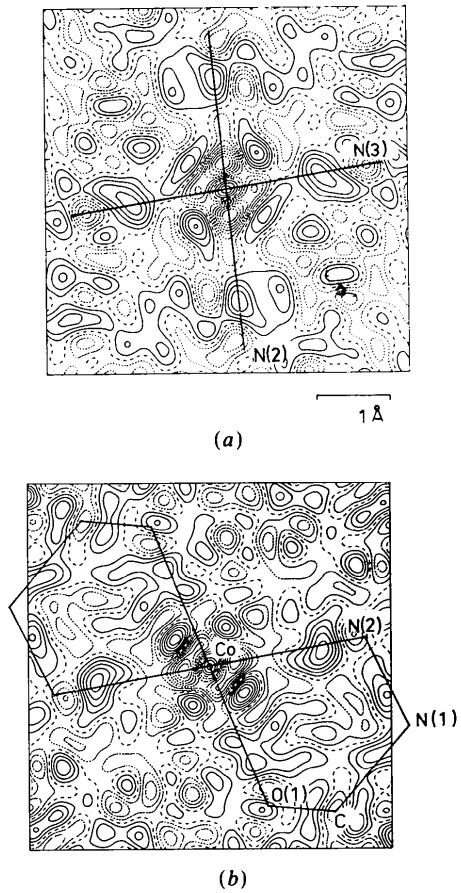

Fig. 3. Difference electron density in planes containing the Co and ligand atoms. Contour interval 0·1 e Å^{-3}. Negative contours broken. (*a*) Section with four N atoms; (*b*) section with two N and two O atoms.

for which charge-density studies have been reported by Marumo, Isobe, Saito, Yagi & Akimoto (1974) and by Marumo, Isobe & Akimoto (1977). The geometries of the structures become progressively farther from ideal through the series M = Ni, Co, Fe. The satellites are very weak in the Ni complex. In the Fe complex, which has a more distorted geometry, the d-electron maxima show a pronounced difference in height, and there are strong satellites associated with the larger maxima.

The development of the satellite peaks may be related to the requirements of the state function for ideal and non-ideal geometries. An atomic $3d$ function has a single maximum in the radial direction. Except for the node at the origin there are no radial nodes in the $3d$ density function. This is characteristic of the densities observed for transition-metal complexes with nearly ideal geometries.

For structures with non-ideal geometries s- and p-type contributions to the valence density may occur. These terms have more radial structure than $3d$ functions, accounting for the subsidiary maxima in $\Delta\rho$ maps for these less-symmetrical structures.

A Perkin–Elmer 3240 computer was used for all calculations. Standard programs from the *XTAL* system (Stewart & Hall, 1985) were used in the structure refinement and for evaluating the difference density. Financial support for this project was provided by the Australian Research Grants Scheme and by the Research Committee of the University of Western Australia. One of us (SCR) acknowledges receipt of a Commonwealth Postgraduate Award.

References

CHANTLER, C. (1985). *PARTN*. Listing and documentation. Unpublished.

HIRSHFELD, F. (1977). *Theor. Chim. Acta*, **44**, 129–138.

International Tables for X-ray Crystallography (1974). Vol. IV. Birmingham: Kynoch Press. (Present distributor D. Reidel, Dordrecht.)

IWATA, M. & SAITO, Y. (1973). *Acta Cryst.* B**29**, 822–832.

KIJIMA, N., TANAKA, K. & MARUMO, F. (1981). *Acta Cryst.* B**37**, 545–548.

KIJIMA, N., TANAKA, K. & MARUMO, F. (1983). *Acta Cryst.* B**39**, 557–561.

MARUMO, F., ISOBE, M. & AKIMOTO, S. (1977). *Acta Cryst.* B**33**, 713–716.

MARUMO, F., ISOBE, M., SAITO, Y., YAGI, T. & AKIMOTO, S. (1974). *Acta Cryst.* B**30**, 1904–1906.

MASLEN, E. N., RASTON, C. L., SKELTON, B. W. & WHITE, A. H. (1975). *Aust. J. Chem.* **28**, 739–744.

MASLEN, E. N., RIDOUT, S. C. & WATSON, K. J. (1987). In preparation.

MASLEN, E. N., SPADACCINI, N. & WATSON, K. J. (1983). *Proc. Indian Acad. Sci.* **92**, 443–448.

MASLEN, E. N., SPADACCINI, N., WATSON, K. J. & WHITE, A. H. (1986). *Acta Cryst.* B**42**, 430–436.

MIYATA, N., TANAKA, K. & MARUMO, F. (1983). *Acta Cryst.* B**39**, 561–564.

OHBA, S. & SAITO, Y. (1984). *Acta Cryst.* C**40**, 1639–1641.

OHBA, S., SATO, S., SAITO, Y., OHSHIMA, K.-I. & HARADA, J. (1983). *Acta Cryst.* B**39**, 49–53.

REES, B. (1977). *Isr. J. Chem.* **16**, 180–186.

SPACKMAN, M. A. & MASLEN, E. N. (1986). *J. Phys. Chem.* **90**, 2020–2027.

STERNHEIMER, R. (1950). *Phys. Rev.* **78**, 235–243.

STEVENS, E. D. & COPPENS, P. (1979). *Acta Cryst.* A**35**, 536–539.

STEWART, J. M. & HALL, S. R. (1985). *The XTAL System of Crystallographic Programs*. Tech. Rep. TR-1364.1. Computer Science Center, Univ. of Maryland, College Park, Maryland.

TREFRY, M. G., MASLEN, E. N. & SPACKMAN, M. A. (1987). *J. Phys. C*, **20**, 19–28.

VARGHESE, J. N. & MASLEN, E. N. (1985). *Acta Cryst.* B**41**, 184–190.

Acta Cryst. (1987). B**43**, 356–368

Structural Analysis of the Incommensurate and Lock-in Phases of Tetramethylammonium Tetrachlorozincate(II), $[N(CH_3)_4]_2[ZnCl_4]$

BY G. MADARIAGA, F. J. ZUÑIGA, J. M. PÉREZ-MATO AND M. J. TELLO

Departamento de Física, Facultad de Ciencias, Universidad del Pais Vasco, Apdo 644, *Bilbao, Spain*

(*Received* 29 *September* 1986; *accepted* 12 *February* 1987)

Abstract

The structures of the incommensurate and lock-in phases of $[N(CH_3)_4]_2[ZnCl_4]$ have been determined and analysed in terms of symmetry modes. X-ray diffraction intensities of the incommensurate phase, including first- and second-order satellites, were collected at 286·4 K. Refinements were performed in the superspace group $P(Pmcn)$:$(s, 1, -1)$ including in the modulation function harmonics up to second order. From a total of 475 independent reflections, final R values of 0·077, 0·052, 0·121 and 0·49 for all, main, first- and second-order reflections, respectively, were obtained. First-order harmonics dominate in the modulation, the most important component of the distortion being that parallel to the a axis. The refinements of the lock-in ferroelectric structure were performed in the space group $P2_1cn$, using as starting parameters those of the basic structure extended to five cells. A final $R = 0{\cdot}075$ for 917 observed reflec-

0108-7681/87/040356-13$01.50